Plant-microbe-mediated decrease of greenhouse gases under dynamic wetland hydrology

Regina B. Bledsoe, Colin G. Finlay*, Ariane L. Peralta

Department of Biology, East Carolina University, Greenville, NC 27858, USA

*Corresponding author: telephone: +1 307.690.1734, e-mail: finlayc21@students.ecu.edu

Regina B. Bledsoe and Colin G. Finlay are co-first authors.

Abstract

While wetlands represent a small fraction (~5-10%) of the world's land surface, it is estimated that one third of wetlands have been lost due to human activities. Wetland habitat loss decreases ecosystem benefits such as improving water quality and mitigating climate change. These microbially mediated functions are dependent on redox conditions, which are altered by soil hydrology and the presence of plants. In this study, we hypothesized that redox status due to continuous flooding would support greater abundance of microbial taxa involved in methanogenesis (obligate anaerobes), but plant-mediated oxygen transport would decrease methane emissions. Using a mesocosm design, we manipulated the duration of hydrologic conditions (i.e., stable dry, stable flooding, and alternating wet/dry) and presence of plants to induce soil redox changes in wetland soils. We measured soil redox status, used targeted amplicon and shotgun metagenomic sequencing to characterize microbial communities, and measured greenhouse gas production to assess microbial function. Results showed that hydrologic history influenced microbial community composition while plant presence and hydrologic treatment altered microbial functional gene composition to a lesser degree. Plant presence decreased greenhouse gas production while differences in the community composition of functional genes related to carbohydrate metabolism, denitrification, and methanogenesis also explained variation in emissions of carbon dioxide and to a lesser extent, methane. While previous studies do not often include plants when assessing greenhouse gas emissions, this study highlights that plant-mediated decreases in greenhouse gas emissions are important and plant-mediated effects should be considered when estimating the carbon balance of ecosystems.

Importance

This study revealed that initial hydrologic conditions (compared to manipulated hydrology) strongly influenced microbial community composition more than function. Specifically, results showed that hydrology is a strong environmental filter that determines microbial taxonomic and functional community patterns, short-term redox changes that are most distinct from historic redox conditions shift microbial communities, and plant presence can stabilize redox shifts and mediate greenhouse gas production. These results highlight the importance of plant presence and the duration of flooding and drying periods to wetland greenhouse gas production.

Introduction

Wetlands represent only 5-10% of terrestrial land surface (1); however, it is estimated that we have lost at least 21% of wetlands as of 2023 (2). Loss of important functions is a consequence of land use conversion of wetlands to urban and agricultural development. These wetland ecosystems provide valuable services such as improving water quality by decreasing nutrient and pollutant loads and mitigating climate change by sequestering carbon. Therefore, there is an interest in conserving, restoring, and constructing wetlands for these ecosystem benefits. Examples of valuable wetland ecosystem functions are anaerobic microbial processes associated with saturated soils that promote complete inorganic nitrogen removal via denitrification ($NO_3^- \rightarrow N_2$) and suppress aerobic decomposition of organic matter. These same anoxic soil conditions can also support methane (CH_4) production (via methanogenesis), which could decrease long-term carbon storage and climate change mitigation benefits of wetlands. Microbial functions associated with delivery of ecosystem services have the potential to be managed to enhance beneficial wetland services (3). To achieve microbial management, a deeper understanding of the controls on wetland microbial ecosystem functions is needed.

To produce cellular energy, adenosine triphosphate (ATP), microorganisms catalyze a series of oxidation-reduction (redox) reactions. Aerobic respiration yields the greatest amount of energy and is expected under dry conditions; but as water fills soil pore spaces, diffusion of oxygen (O_2) into the soil matrix decreases, causing a shift to a reducing environment (4, 5). Reducing environments favor anaerobic respiration in which other molecules such as nitrate (NO_3^-), manganese, ferric iron, sulfate, and carbon dioxide (CO_2) are used as terminal electron acceptors (6). As soil moisture increases, O_2 availability and soil redox potentials decrease, which corresponds to a shift in available electron acceptors (4). Redox potentials measured between +600 and +250 mV are considered oxidative conditions while redox potentials measured from +250 to -400 mV are considered reducing conditions (4). Therefore, measuring soil redox potential

is useful for predicting which biogeochemical processes are likely to be carried out by soil microbes.

To manage microbial functions in support of nitrogen removal and retention but with decreased CH_4 production, a better understanding of the extent to which the presence of vegetation and changes in hydrology (e.g., flooding, drying) affect microbial communities is needed. Complex interactions between abiotic factors, such as soil physicochemical properties, redox status and nutrient availability, and biotic factors, including abundance of vegetation and microbial community structure, influence microbial functions to varying degrees. A microbial community is composed of many taxa with varying physiologies which respond differently to changes in the local environment (7, 8). Particular microbes may be more adapted to specific hydrologic conditions in their environment, where only a subset of microbial taxa can persist in response to frequent changes in soil moisture (4, 9). However, unexpected microbial responses can also occur due to dormancy of soil bacterial taxa (10, 11). As such, hydrologic changes in wetlands due to drought, draining, and re-wetting cause shifts in soil redox potentials and microbial community composition and metabolism, which can influence the relative rates of anaerobic processes such as denitrification and methanogenesis (4, 9, 12).

If drying and re-wetting events are periodic, a cycle of activity and dormancy can maintain high microbial diversity compared to more stable environmental conditions (9). For example, denitrifiers are facultative anaerobes and are capable of using O_2; but in anoxic conditions, denitrifiers can switch to reducing NO_3^- to nitrous oxide (N_2O) and dinitrogen (N_2) gas during respiration (13). In addition, methanogens are dominant in the most anoxic conditions such as flooded wetlands, and are responsible for converting CO_2 to CH_4 (13). Fluctuating hydrologic conditions can shift the microbial community to one that can only tolerate transitional zones. As hydrologic changes occur, oxic-anoxic interfaces provide environmental conditions that sometimes support methanotrophs that convert CH_4 to CO_2 and denitrifiers (13–15). Therefore, the availability of electron acceptors (e.g., O_2, NO_3^-) in the soil environment influences the relative

abundance of microbial functional groups (i.e., subset of microbes capable of using a suite of electron acceptors) and rates and types of microbial processes.

While hydrology is a primary determinant of soil redox potential, plants also modify the soil environment. The soil microenvironments that are in contact with plant roots are hotspots of microbial activity due to plant-mediated transport of nutrients, O_2, and carbon belowground (16–18). Plants can also transport CH_4 aboveground through aerenchyma in shoots. Also, radial O_2 loss from plant roots can increase soil redox potentials around the root zone producing microenvironments that can support aerobic microbial processes (18). Additionally, vegetation can alter soil redox potentials by facilitating transport of O_2 into roots zones (18, 19) and transporting CH_4 from root zones into the atmosphere (20, 21).

The aim of this study is to provide insight into how the duration of hydrologic change (i.e., sustained dry, interim dry/wet, sustained wet), and the presence of vegetation in wetland soils change the structure of the microbial community, redox conditions, and greenhouse gas (GHG) production. We hypothesize that dry and dry/wet transition conditions will support similar microbial communities, but that redox potentials and GHG production rates will differ between manipulated hydrologic treatment conditions. We expect that dry conditions with and without vegetation will support higher redox potentials (i.e., oxidative conditions) and a higher rate of CO_2 production with some N_2O production but little or no CH_4 production. We expect this because dry and transition conditions should support similar communities of facultative anaerobes that can switch between respiration pathways depending on current soil saturation levels. Additionally, in dry conditions soils are already aerated so plant-mediated gas transport belowground should not alter redox potentials. However, in fluctuating wet conditions, we expect that redox conditions will shift between oxidative and reducing conditions due to soil saturation. Also, plant presence is expected to increase redox potentials during saturated periods, due to plant-mediated gas transport belowground, compared to treatments where vegetation is absent. Due to lower O_2 levels when saturated conditions are present, we expect decreased CO_2 production but increased nitrous

oxide production with plants due to plant stimulation of denitrification via organic matter inputs and elevated O_2 supporting nitrification to supply NO_3^- to denitrifiers (22). Also, in the presence of plants, and in dry/interim conditions, we expect CH_4 production will be lower due to methanogens being obligate anaerobes. Flooded conditions will support different microbial communities than dry or fluctuating environments due to consistently low redox potentials (i.e., reducing conditions) resulting in the highest rates of CH_4 production and complete denitrification rates since these are both anaerobic processes. Although, other studies (20, 21) have found increased methanogenesis in the presence of some plant species, in the present study, we expect that soils with plants will have lower CH_4 production compared to flooded soils without plants. This is expected due to O_2 transport from roots supporting aerobic methanotrophic microbial taxa that consume CH_4.

To test these hypotheses, we conducted a mesocosm experiment in which we manipulated hydrology (i.e., dry, interim, and wet) and presence of plants in soils collected from different hydrologic histories (i.e., dry, wet/dry transition, and saturated wet zones) within a restored coastal plain wetland. We measured soil nutrient concentrations, redox potentials, GHG concentrations and characterized soil microbial communities using 16S rRNA gene amplicon sequencing. By simulating acute differences in hydrologic states, the addition of plants, and maintenance of soil structure, we were able to link microbial-scale changes to ecosystem-level processes.

Methods

Study site

We collected soil samples from the Timberlake Observatory for Wetland Restoration located in the Albemarle Peninsula in Tyrell County, North Carolina (35°54’22” N 76°09’25” W; Fig. 1). Previously described by (23) and (24), the field site is part of the Great Dismal Swamp Mitigation Bank, LLC which is a 1,700 ha wetland consisting of 420 ha of mature forested wetland, 787 ha

of forested wetland, 57.2 ha of drained shrub-scrub, and 440 ha of agricultural fields restored to wetland habitat in 2007 (23, 25). A major portion of the restoration effort was to remove drainage ditches and plant 750,000 saplings including *Taxodium distichum, Nyssa* spp., *Salix nigra, Fraxinus pennsylvanica, and Quercus* spp. (24). A more recent survey indicates that the dominant plant species at the site is *Juncus effusus* L. along with *Euthamia caroliniana* (L.) Greene ex Porter & Britton, *Solidago fistulosa* Mill., and *Scirpus cyperinus* (L.) Kunth (26). The site is connected to the Albemarle Sound via the Little Alligator River, and the site's position in the landscape increases the potential for saltwater intrusion to occur. In addition, salinity in the sound ranges from 0-7 psu and up to 12 psu during drought years (25). Even though there is little elevation change (-1 m to 2 m) across the restored wetland, there is a hydrologic gradient, which is driven by the position of the water table and represents upland dry, saturated wet, and transition dry/wet sites (26).

Mesocosm experimental design

We used a mesocosm approach to assess the changes in the soil microbial community, redox potentials, and GHG production due to hydrologic changes and vegetation. We set up a mesocosm experiment using soil blocks collected from three sites within the Timberlake Observatory for Wetland Restoration field site. Soils were collected from the restored (12 years post-restoration) portion of the site that was previously used as agricultural fields for several decades prior to restoration (23). We collected soils that represented three different hydrologic zones on the inflow side of the site at the following coordinates: 35°53'45.3"N 76°09'57.5"W (dry), 35°53'44.8"N 76°09'57.1"W (dry/wet transition or interim), and 35°53'44.3"N 76°09'56.0"W (wet). Six intact soil blocks (25 cm × 25 cm × 20 cm deep) were cut out from each of the three sites using landscaping knives and shovels. Soil history was determined by water table levels at the time of collection (dry = 20 cm, interim = 10 cm, and wet = 0 cm below surface level). Soil blocks were contained in dark plastic containers of the same dimensions as the soil blocks (Fig. 1). To

manipulate hydrology within the mesocosm, vinyl tubing was inserted 3 cm from the bottom of the mesocosm container on each side and connected to a 1 L water bottle (Fig. 1). Water levels inside the mesocosm were maintained by filling the 1 L bottle to the desired height using rainwater collected from a cistern. To manipulate the presence of vegetation, the mesocosm was divided in half and separated by root screen (20 µm stainless steel mesh). On one side plants were allowed to grow during the experiment, while the 'no plant' side was maintained by careful removal of above- and belowground plant biomass. Finally, 4" schedule 40 polyvinyl chloride (PVC) collars were inserted 5 cm below the surface as a sampling base for GHG chambers (described in subsection *GHG concentrations*). The mesocosm experiment was housed at the East Carolina University West Research Campus (Greenville, NC) under a covered hoop house with shade cloth which prevented precipitation and allowed 60% light into the hoop house. Soils were collected April 1, 2016, prepared on May 29, 2016, and experimental mesocosm sampling started on June 13, 2016, and ended on August 11, 2016. Temperatures ranged from 22.7 °C ± 1.5 to 30.8 °C ± 1.4 during the experimental sampling period. Because the hoop house was in a wetland about 100 miles from the field site (within same physiographic region), temperature and relative humidity in the hoop house would have resembled field conditions, and the blocking of precipitation was essential for controlled manipulation of hydrologic conditions.

Two weeks after installing PVC collars and setting up the plant treatment, we started hydrologic treatments. Hydrologic manipulation occurred over eight weeks to allow for multiple dry/wet transitions for the interim treatment. Mesocosms exposed to wet conditions were flooded by overhead watering and maintained using water reservoirs filled to maximum container height (18 cm). Mesocosms exposed to dry conditions were maintained using water reservoirs filled to 5 cm. The dry/wet (interim) treatments fluctuated between flooded and dry conditions, as described above, every two weeks starting with a wet treatment and ending with a dry treatment. We measured soil redox status and microbial community composition at the beginning and end of the eight-week experiment. In addition, we measured GHG fluxes every two weeks starting two

weeks after initiating hydrologic treatments. Finally, at the end of the eight-week experiment, we collected soils for physiochemical analyses: soil moisture, pH, total carbon, total nitrogen, extractable ammonium (NH_4^+) and NO_3^-, phosphorus, potassium, magnesium, sulfur, iron, manganese, and organic matter concentrations (described in subsection *Soil Physiochemical Characteristics*).

Measuring integrated soil redox status

We measured soil redox status at the beginning and end of the hydrologic experiment using Indicator of Reduction in Soils (IRIS) tubes (InMass Technologies; (27) (Fig. 2; Fig. S1). The IRIS tubes are constructed from 1/2" schedule 40 PVC pipe coated in iron oxide (Fe(III)) paint (28). When exposed to oxidative conditions, Fe(III) is visible as an orange-red paint; but when exposed to anoxic conditions, Fe(III) is reduced to Fe(II) which dissolves in solution and appears as a clearing (white) on the tube (27, 28). At the beginning of the experiment, two IRIS tubes (12 cm depth) were installed in each mesocosm: one on the plant side and one on the bare soil side. The IRIS tubes were incubated in mesocosm conditions for two weeks before removal and analysis. After we removed the IRIS tube, a non-coated PVC pipe was used to fill the hole. Two weeks prior to the end of the experiment, the non-coated PVC pipe was removed and replaced with a new IRIS tube to measure soil redox status at the end of the experiment.

We quantified the surface area of Fe(III) paint removed from IRIS tubes using ImageJ software (v1.48, (29)). First, we imaged the entire tube by taking four pictures and then stitched the photo into a composite using GIMP2 (v2.8.14, https://gimp.org/) photo editing software. Next, we identified areas of artificial paint removal, that is scratches from installing or removing tubes, and manually filled these pixels. Then, using ImageJ software (v1.48, (29)), we converted all colored pixels to black. We compared the number of white pixels to total pixels to determine the percent of paint removed. Interpretation of redox status is based on the percent paint removed from a 10 cm section of tubing and summarized as follows: 0% not reducing, 1-5% probably not

reducing, 5-10% possibly reducing, 10-25% and >25% definitely reducing (28). For regression analysis of GHG concentrations as a function of redox status, percent of paint removed was treated as a continuous variable to represent redox status.

Soil physiochemical characteristics

Soil proprieties were determined from soils collected during the destructive sampling of mesocosms at the end of the experimental duration. We collected six soil cores (3 cm diameter, 10 cm depth) from each side of the box (i.e., plant and no plant) and combined cores collected from one side into a composite sample (i.e., one plant composite and one no plant composite), passed soils through a 4 mm sieve, and homogenized samples prior to subsampling for soil analyses. For each sample, we measured gravimetric soil moisture by drying 20-30 g of field-moist soil at 105 °C for at least 24 hours. Approximately 5 g of field moist soil was extracted with 45 ml of 2 M KCl, and extractable NH_4^+ and NO_3^- ions were colorimetrically measured using a SmartChem 200 auto analyzer (Unity Scientific Milford, Massachusetts, USA) at the East Carolina University Environmental Research Laboratory. To determine total carbon and total nitrogen (TC, TN), a subsample of air-dried soil was finely ground and sieved through a 500 µm mesh and analyzed using an elemental analyzer (2400 CHNS Analyzer; Perkin Elmer; Waltham, Massachusetts, USA) at the Environmental and Agricultural Testing Service Laboratory, Department of Crop and Soil Sciences, North Carolina State University. A second subsample of air-dried soil was sent to Waters Agricultural Laboratories, Inc. (Warsaw, NC) and analyzed for pH, phosphorus, potassium, magnesium, sulfur, manganese, iron, and humic matter, using standard Mehlich III methods (30, 31).

Greenhouse gas (GHG) concentrations

We examined the effects of hydrology and vegetation on GHG production. We measured GHG concentrations on June 13, 2016, two weeks after hydrologic treatments were established,

and then every two weeks until August 11, 2016, for a total of five sampling events. The GHG collection chambers were 20 cm in height with a diameter of 8.25 cm and constructed from clear acrylic tubing. Since GHG samples were captured using clear chambers versus opaque chambers, GHG measurements represent total GHG fluxes and not just soil respiration due to microbial activity. Chambers were sealed on one end with silicon and a pipe cap with 33 mm septa installed as gas sampling port. At the time of sampling, chambers were placed on top of preinstalled PVC collars and the seals were taped to prevent diffusion from the seam (32). A gas sample was collected from chambers at each of the following four time points: 30 minutes, 60 minutes, 120 minutes, and 180 minutes post-chamber attachment. To collect gas samples, we used a needle attached to a 20 mL syringe, mixed headspace gas three times by pulling and depressing the plunger, and then collected 20 mL of sample. The collected gas sample was equally distributed between two 3 mL glass Exetainer vials (Lampeter, Wales, UK) fitted with screw top and dual layer septa. Samples were stored upside down at room temperature in a dark location and were analyzed within 96 hours of collection. We analyzed GHG concentrations using a Shimazdu gas chromatograph (GC-2014) fitted with an electron capture detector to detect N_2O and flame ionization detector with methanizer to measure CH_4 and CO_2. Calibration standards for June 13 and June 28, 2016, contained 0, 120, 240, 360, and 480 CO_2 parts per million (ppm); 0, 1, 2, 3, 4, and 5 CH_4 ppm; 0, 0.2, 0.4, 0.6, 0.8, and 1 N_2O ppm. Calibration standards for July 11, Jul 25, and August 11, 2016, contained 0, 120, 480, 1200, 2400, and 3000 CO_2 ppm; 0, 1, 4, 20, 40, and 50 CH_4 ppm; 0, 0.2, 0.8, 20, 40, and 50 N_2O ppm. If a sample measured above the calibration curve, we diluted the sample and reanalyzed it.

We used the linear change in concentration and the ideal gas law to calculate GHG fluxes (33, 34). However, upon curation of analyzed gas samples for GHG flux calculations, we identified that 30-50% of samples from no plant treatments were not linear and that 50-75% of those samples represented wet treatments. We also observed a high proportion of negative fluxes (Fig. S2). Both the nonlinear and negative fluxes are indicative of chamber leakage (35).To

accommodate chamber leakage, a nonlinear flux calculation when used when possible (35). Linear and robust linear fluxes were calculated when a nonlinear calculation was not possible, but a high proportion of negative fluxes remained (Fig. S2). Due to the statistical power lost in determining the effects of hydrology and plants on GHG rates by removing these samples from further analyses, we chose an alternate approach to analyzing gas samples. We determined the concentration of CH_4, CO_2, and N_2O in each sample for the first sampling time point which occurred at the first 30-minute collection interval. To evaluate the explanatory power of this approach, we examined the relationship between CO_2 flux and the first timepoint of GHG fluxes from a different project. We measured monthly GHG fluxes at a long-term nutrient and disturbance by mowing experiment in an eastern North Carolina coastal plain wetland described in Bledsoe et al. 2020 (36) and Goodwillie et al. 2020 (37). The experiment examined fertilization and disturbance by mowing effects on *in situ* soil GHG emissions using monthly fixed chamber GHG flux measurements over 18 months. We considered unmowed and unfertilized plots with wet conditions the most similar to field conditions in the present study, and therefore, only used GHG data from these plots in the following regression analysis. The flux consisted of four timepoints (T_0-T_3) starting at time = 0 with 15-minute intervals between timepoints. Linear regression, CO_2 flux ~ concentration at T1, revealed a positive relationship, with concentration at T1 explaining 20% of the variance in CO_2 flux ($F_{1,27}$ = 8.21, R_{adj}^2 = 0.20, P = 0.008, Fig. S3). Based on this analysis, we conclude that patterns in T1 in the present study resemble patterns in GHG flux and T1 explains 20% of variance in fluxes that would have been measured without chamber leakage.

Bacterial and archaeal community analyses

We assessed the soil microbial community composition at the beginning of the experiment ('start' based on soils collected from the IRIS tube installation) and at the end of the experiment ('final' based on soils collected during destructive sampling). We collected 'final' soil samples using a standard soil probe (3 cm diameter, 10 cm depth) from the same location that we collected

GHGs samples. We extracted genomic DNA from soils using the Qiagen DNeasy PowerSoil Kit and diluted DNA to 20 ng μl^{-1}. This genomic DNA was used as template in PCR reactions and used barcoded primers (bacterial/archaeal 515FB/806R primer set) originally developed by the Earth Microbiome Project (38) to target the V4 region of the bacterial 16S subunit of the ribosomal RNA gene (38–40). For each sample, three 50 µL PCR libraries were prepared by combining 35.75 µL molecular grade water, 5 µL Amplitaq Gold 360 10x buffer, 5 µL $MgCl_2$ (25 mM), 1 µL dNTPs (40mM total, 10mM each), 0.25 µL Amplitaq Gold 360 polymerase, 1 µL 515 forward barcoded primer (10 µM), 1 µL 806 reverse primer (10 µM), and 1 µL DNA template (10 ng μL^{-1}). Thermocycler conditions for PCR reactions were as follows: initial denaturation (94 °C, 3 minutes); 30 cycles of 94 °C for 45 seconds, 50 °C for 30 seconds, 72 °C for 90 seconds; final elongation (72 °C, 10 minutes). The triplicate 50 µL PCR libraries were combined and then cleaned using the Axygen® AxyPrep Magnetic (MAG) Bead Purification Kit (Axygen, Union City, California, USA). Cleaned PCR products were quantified using QuantIT dsDNA BR assay (Thermo Scientific, Waltham, Massachusetts, USA) and diluted to a concentration of 10 ng μL^{-1} before pooling libraries in equimolar concentration of 5 ng μL^{-1}. We sequenced the pooled libraries using the Illumina MiSeq platform using paired end reads (Illumina Reagent Kit v2, 500 reaction kit) at the Indiana University Center for Genomics and Bioinformatics Sequencing Facility.

Sequences were processed using the mothur (v1.42.0) (41) MiSeq pipeline (42). We assembled contigs from the paired end reads, quality trimmed using a moving average quality score (minimum quality score 35), aligned sequences to the SILVA rRNA database (v132) (43), and removed chimeric sequences using the VSEARCH algorithm (44). We created operational taxonomic units (OTUs) by first splitting sequences based on taxonomic class and then binning into OTUs based on 97% sequence similarity. Taxonomic identity was assigned using the SILVA rRNA database (v132) (43). Since amplicon sequencing was conducted using short-reads (250 bp) and not assembled genomes, we used an OTU-based 3% distance threshold to avoid splitting the same bacterial genome into distinct clusters (using amplicon sequence variant (ASV) of a

single base difference). An OTU-based approach also limits over-inflated numbers of ASVs introduced by PCR bias and sequencing errors (45). In addition, employing an OTU- or ASV-based approach is known to result in similar broadscale community composition patterns (46).

Shotgun metagenomic analyses

Based on amplicon sequencing, we identified a subset of samples representing the most distinct microbial communities for shotgun metagenomic sequencing. Description of sample processing and metagenomic sequencing can be found in Peralta et al. (2020) (47). Briefly, we chose a set of baseline and post-flooding/drying treatment samples. We sourced mesocosm baseline conditions from relatively drier field locations (water level at about -20 cm, n = 4) and relatively wetter plots (water level at about 0 cm, n = 4). At the end of the eight-week experiment, we selected a subset of samples from the hydrologic treatments (prolonged drying or wetting only) and plant treatments (presence or absence of vegetation) (n = 16). After genomic DNA extraction using the Qiagen DNeasy PowerMax soil kit, samples were sent to the U.S. Department of Energy (DOE) Joint Genome Institute (JGI) for sequencing and analysis (GOLD study ID Gs0142547 and NCBI BioProject accession number PRJNA641216). Plate-based DNA library preparation and subsequent Illumina sequencing, according to published protocols (47), resulted in 583.2 Gbp of raw sequence data. Raw data were processed using the DOE JGI Metagenome Annotation Pipeline IMG/M v.5.0.9 (48–50).

From the metagenomes, we curated functional gene sets using IMG/M's integrated Kyoto Encyclopedia of Genes and Genomes (KEGG) module list. For statistical analyses, we focused on the following four functional gene sets associated with biogenic greenhouse gas concentrations of N_2O, CH_4, and CO_2: (1) Denitrification (KEGG Module M00529), (2) Methanogen (M00617), (3) Central Carbohydrate Metabolism (M00001-M00011, M00307-M00309, M00580, and M00633), and (4) Prokaryotic Cytochrome C Oxidase (CcO) (M00155).

Statistical Analyses

All statistical analyses were performed in the R statistical environment (RStudio 2022.12.0+353, Rv4.3.3) (51). Prior to multivariate statistical analyses, we normalized sample-to-sample variation in sequence depth by taking the relative abundance of each OTU: dividing the count of each OTU by the total number of OTUs for each soil community. OTU data were then rarefied using vegan::rrarefy, producing randomly sampled subsets of OTUs with each sample having an equal number of unique OTUs (52). Likewise, functional gene counts were converted to relative abundance by dividing the count of each functional gene by the total number of functional gene counts in each respective functional gene category. We examined beta diversity by visualizing bacterial community responses to hydrologic history (field conditions), hydrologic treatment (contemporary dry/wet treatments), and plant presence/absence using principal coordinates analysis (PCoA) of bacterial community composition based on Bray-Curtis dissimilarity. We also used PCoA to visualize composition (Bray-Curtis dissimilarity) of functional gene categories according to hydrologic history, hydrologic treatment, plant presence/absence, and baseline (sampled before beginning hydrologic and plant treatments). We used permutational multivariate analysis of variance (PERMANOVA) to determine differences between bacterial communities among hydrologic history, hydrologic treatment, and plant presence. Hypothesis testing using PERMANOVA was performed using the *vegan::adonis* function (52). Unique taxa representing each hydrologic history and hydrologic treatment were determined by Dufrene-Legendre indicator species analysis using the *labdsv::indval* function (53). Finally, soil parameters were compared against bacterial community and functional patterns (based on Bray-Curtis dissimilarity) using *vegan::envfit* function (52). Soil parameters with $p \leq 0.05$ were represented on the PCoA plot of 16S rRNA community composition as vectors scaled by their correlation to microbial community patterns. The GHG concentrations with *envfit* $p \leq 0.1$ were plotted as vectors, scaled by their correlation, on PCoA plots of functional gene composition.

We constructed linear mixed effects models with sampling plot and sampling date as random effects to determine the importance of the fixed effects of hydrologic history (field conditions), hydrologic treatment (contemporary dry/wet treatments), and plant presence on GHG concentrations using the *lme4* R package (54). The CH_4, CO_2, and N_2O concentrations were log transformed to better meet normality assumptions prior to running mixed effects models. Then, we used Akaike's Information Corrected Criterion (AICc) model comparisons, which adjust for small sample size, against the null model to determine which simplest combination of fixed effects (hydrologic history, hydrologic treatment, and plant presence) is needed to explain the most variation in GHG concentrations (55, 56). We compared individual fixed effects and the combination of those fixed effects. We did not use the interaction between the fixed effects hydrologic history and hydrologic treatment because combinations would have resulted in a sample size of $n = 2$ for each group. Lastly, to determine the proportion of variance explained by fixed effects (marginal) and the complete model (conditional), we used the *MuMIn* R package (56, 57).

While linear mixed effects models are robust to departures from normality (58), traditional ANOVAs and t-tests are less so (59, 60). To accommodate extreme outliers and lack of normality, we used nonparametric statistics to test for differences in GHG concentrations among hydrologic treatments, and plant presence/absence. We used Wilcoxon Rank Sum tests to evaluate differences in GHG concentrations among plant versus no plant groups. To accommodate repeated measures without pseudoreplication, Wilcoxon Rank Sum tests were blocked by sampling date. We used Kruskal-Wallis Rank Sum tests to examine differences in GHG concentrations among the three hydrologic treatments (dry, interim, and wet). To accommodate repeated measures, Kruskal-Wallis tests were grouped by sampling date. If the Kruskal-Wallis test for a sampling date revealed differences among treatment groups ($p \leq 0.05$), we then performed a pairwise comparisons using the Dwass, Steel, Critchlow, and Fligner (SDCFlig) test with a Monte Carlo distribution (61).

To assess microbial community structure and function relationships, we examined the relationship between individual GHG concentrations and microbial community/functional Bray-Curtis dissimilarity matrices using distance-based partial least squares regression (DBPLSR) in the *dbstats* R package (62). Finally, we used Mantel r statistic function in the *vegan* R package (52) to examine the relationship between the soil properties (redox, percent moisture, pH, NH_4^+, total soil C, phosphorus ppm, potassium ppm, magnesium ppm, sulfur ppm, and percent humic matter) and microbial community composition. Only soil properties with a correlation of < 50% were used in this analysis.

Data Availability

All code and data used in this study are in a public GitHub repository (https://github.com/PeraltaLab/WetlandMesocosm_GHG_Timberlake), Raw amplicon sequence files can be found at NCBI SRA BioProject ID PRJNA636184, and metagenome sequence files can be found at NCBI SRA BioProject ID PRJNA641216.

Results

Soil mesocosms sampled from the Timberlake Observatory for Wetland Restoration, in three distinct hydrologic conditions (dry, interim, wet) (Fig. 1A), were subjected to eight weeks of hydrologic and plant presence/absence treatments (Fig. 1B). The three levels of eight-week hydrologic treatments were: (1) flooded for eight weeks, (2) dry for eight weeks, and (3) interim, i.e., two weeks flooded alternating with two weeks dry for a total of eight weeks. Each box was separated by a stainless mesh divider, with plants allowed to grow on one side, and plants removed on the other side (Fig. 1B).

Characterization of soil physical-chemical properties

There was little variability in soil properties across main effects (hydrologic history, hydrologic treatment, plant presence), with the exception of notable differences in soil moisture between plant treatments within dry and wet hydrologic treatments (Table 1). In addition, NO_3^-N concentrations were below detection limits in samples with plants, but concentrations were measurable in samples without plants (0.01 ± 0.0005 to 0.25 ± 0.38 NO_3^-N mg L^{-1}) (Table 1). Soil redox status as measured by IRIS tube analysis revealed that soils experiencing dry and interim treatments (0% iron oxide paint removed) were not reducing, while soils in wet treatments were reducing (average 40%, range 27-67% paint removed) (Fig. 2). In wet treatments, plant presence decreased soil redox status to a lesser degree (average 38%, range 27%-60% paint removed) than when plants were absent, but soils were still considered reducing (Fig. 2, Fig. S1).

Plant and soil redox effects on greenhouse gas concentrations

Methane (CH_4) – Within no-plant treatments, wet hydrologic treatment (228.72 ± 480.88 ppm CH_4, mean ± standard deviation) produced the highest CH_4 concentrations and the greatest variability between samples compared to dry (66.72 ± 324.58 ppm CH_4) and interim treatments (62.56 ± 251.99 ppm CH_4) (Table S1). However, treatments with plants produced the lowest CH_4 concentrations across wet, dry, and interim hydrologic treatments (7.94 ± 6.79, 4.48 ± 8.92, 10.04 ± 16.68 ppm CH_4, respectively) (Table S1). When comparing plant vs. no plant CH_4 concentrations at each of five timepoints, no differences were detected, except for during the first timepoint on June 13th, where CH_4 concentrations were greater in the absence of plants than the presence of plants (Figure 3, Table S2). There were differences in CH_4 concentrations in the hydrologic treatment groups in each of the five timepoints, except on June 13th (Figure 4, Table S3). The wet treatment produced greater CH_4 concentrations than the dry treatment throughout the final four timepoints (June 18th through August 11th), and differences in wet vs. interim and dry vs. interim were observed but did not persist throughout the experiment (Figure 4, Table S3). The linear mixed-effects model with plant presence, hydrologic treatment, and hydrologic history

explained the most variance in CH_4 concentrations based on ΔAICc score of 0 and AICc weight of 0.65 (Table S4). The full model explained 49% of variance in CH_4 concentrations, while the fixed effect of plant presence/absence explained 27% of the variance, and hydrologic history and hydrologic treatment explained 18% and 16%, respectively (Table S4).

Carbon dioxide (CO_2) – Dry (1056.16 ± 443.75 ppm CO_2), interim (612.93 ± 309.89 ppm CO_2), and wet (478.42 ± 188.7 ppm CO_2) hydrologic treatments with no plants produced greater CO_2 concentrations compared to dry, interim, and wet treatments with plants (451.09 ± 254.66, 365.85 ± 180.18, 314.98 ± 78.7 ppm CH_4, respectively) (Table S1). Specifically, CO_2 concentrations were greater in no plant mesocosms compared to plant mesocosms, except during the second timepoint on June 28th (Figure 3, Table S2). During the third timepoint (July 11th), CO_2 concentrations in the dry treatment exceeded CO_2 concentrations in the wet treatment (W = -3.51, p = 0.03; Figure 4, Table S3). The following month (August 11th), differences in dry vs. wet (W = -3.92, p = 0.01) and interim vs. wet (W = -4.00, p = 0.01) CO_2 concentrations were observed (Figure 4, Table S3). The linear mixed-effects model, which included the additive effects of plant, hydrologic treatment, and hydrologic history, was most plausible, based on a ΔAICc score of 0 and AICc weight of 0.74 (Table S4). The full model explained 55% of variance in CO_2 concentrations, while the fixed effect of plant presence/absence explained 28% of the variance, and hydrologic history and hydrologic treatment explained 19% and 4%, respectively (Table S4).

Nitrous oxide (N_2O) – The N_2O concentrations were near zero in all hydrologic and plant treatments (range: 0.103 – 7.458 ppm N_2O) (Figure 3). On July 11th and July 25th, no plant N_2O concentrations exceeded plant N_2O concentrations (Figure 3, Table S2). The N_2O concentrations were similar among hydrologic treatments, except for interim vs. wet on June 28th (W = 4.25, p = 0.0044). The model with plant and hydrologic treatment was most plausible, based on ΔAICc score of 0 and AICc weight of 0.58 (Table S4). The most plausible model (plant + hydrologic

treatment) explained 10% of variance, while the fixed effect of plant explained 13% of variance and hydrologic treatment explained 14% of variance (Table S4).

Relationship between soil redox conditions and GHG concentrations

We used linear regression to examine the relationship between soil redox status (represented by the percent of paint removed from IRIS tubes) and GHG concentrations. The CH_4 concentrations had a weak but significant positive relationship to redox status ($R^2 = 0.27$, $p < 0.001$) (Table S5, Fig. S4). The CO_2 concentrations had a weak but significant negative relationship with redox conditions ($R^2 = 0.29$, $p < 0.001$), and the N_2O concentrations were not significantly related to redox conditions ($R^2 = 0.05$, $p = 0.098$) (Table S5, Fig. S4).

Patterns in microbial community composition

Sequencing efforts returned a total of 1,570,135 reads and 35,897 operational taxonomic units (OTUs) before removing low abundance sequences occurring less than 10 times or 0.01% in all samples. After removing low abundance sequences, 1,505,797 reads representing 7,026 OTUs were retained after filtering. Within OTUs prior to filtering, 15,582 of those OTUs occurred once and 5,536 occurred twice in all samples. All samples were rarefied to 23,528 reads since this was the lowest read count among all samples.

Bacterial and archaeal community composition clustered by hydrologic treatment within hydrologic history (Fig. 5). The PCoA axis 1 explained 25% and PCoA axis 2 explained 11% of microbial community variance (Fig. 5). We observed that hydrologic history (PERMANOVA, $R^2 = 0.305$, $P = 0.001$) and hydrologic treatment (PERMANOVA, $R^2 = 0.110$, $P = 0.002$) explained variance in microbial community patterns (Fig. 5, Table S6). In contrast, microbial community composition was similar in the presence or absence of plant communities (PERMANOVA, $R^2 = 0.102$, $P = 0.824$) (Table S6). In addition, sulfur concentrations were correlated to soil microbial communities from the wet hydrologic history, pH levels were correlated to microbial communities

from the interim hydrologic history, and total soil C and manganese concentrations were correlated to microbial communities from the dry hydrologic history (Fig. 5). Also, overall patterns in microbial composition and soil properties were significantly correlated (Mantel $r = 0.32$, $p < 0.001$) (Table S7).

Indicator species analysis of the top 2.5% OTUs (by relative abundance at a significance level of $p \leq 0.01$) revealed that 34 OTUs, 21 OTUs, and 38 OTUs represented dry, interim, and wet hydrologic histories, respectively (Table S8). The bacterial phyla *Acidobacteria* (Gp1, Gp2, Gp3, and Gp6) (24%) and *Proteobacteria* (*Alpha*-, *Beta*-, *Delta*-, and *Gammaproteobacteria*) (30%) represented communities from dry hydrologic histories, while the bacterial phyla *Acidobacteria* (Gp1, Gp10, Gp3, and Gp7) (33%) and *Proteobacteria* (Alpha-, Beta-, and *Deltaproteobacteria*) (29%) represented communities from interim hydrologic histories (Table S8). Soils from wet hydrologic histories were represented by *Acidobacteria* (Gp1, Gp2, Gp3) (38%) and *Proteobacteria* (Alpha-, Delta-, and *Gammaproteobacteria* (21%) (Table S4). Finally, microbial taxa putatively associated with methane cycling including the archaeal genera *Methanobacterium* and the bacterial genera *Methylocystis* and *Syntrophobacter* were unique to microbial communities from wet hydrologic histories (Table S8). Fewer indicator OTUs were identified for hydrologic treatments (6 OTUs, and 9 OTUs, for interim, and wet hydrologic treatments, respectively) (Table S9). Only one indicator OTU was found in common among hydrologic histories and hydrologic treatments. Interestingly, this shared OTU, *Reyranella*, was indicative of both dry historical conditions, and wet hydrologic treatment conditions.

Patterns in functional gene composition

Following quality control and filtering of raw metagenomic sequencing data, annotation and gene calling resulted in 600,507 ± 172,049 (mean ± SD) annotated contigs per sample. An average of 998,604 ± 307,431 (mean ± SD) gene features per sample were identified. Of the identified gene features, an average of 232,809 ± 70,486 (mean ± SD) KEGG features per sample

were identified. Among the four curated functional gene sets, central carbohydrate metabolism had the highest average KEGG features per sample (13,145 ± 3,848), followed by methanogenesis (1,434 ± 423), CcO (1,325 ± 398.26), and denitrification (350 ± 111).

The four functional gene categories (denitrification, methanogenesis, central carbohydrate metabolism, and CcO) showed varying responses to plant and hydrologic treatment but no response to interactions between plant and hydrologic treatments. Carbohydrate metabolic composition differed between hydrologic treatment (PERMANOVA, $R^2 = 0.09$, $P = 0.04$) but was similar across plant presence and absence (PERMANOVA, $R^2 = 0.07$, $P = 0.69$) (Table S6). In contrast, the compositions of denitrification genes, methanogenesis genes, and CcO genes were similar across plant presence and hydrologic treatments (PERMANOVA, plant history: NS) (Table S6). Plant presence/absence had no significant impact on the composition of functional genes, which was also observed for 16S rRNA microbial community composition (Table S6).

Based on environmental fitting (vegan::envfit), functional gene composition correlated to carbon losses (CO_2 and CH_4 production). Specifically, CO_2 concentrations correlated to the PCoA ordinations of functional gene composition associated with both denitrification (envfit, $R^2 = 0.25$, $P = 0.05$) and carbohydrate metabolism (envfit, $R^2 = 0.23$, $P = 0.06$) (Fig. 5), while the ordination of the methanogenesis genes had a marginally good fit with CH_4 production (envfit, $R^2 = 0.20$, $P = 0.09$) (Fig. 5).

Relationships between GHG concentrations, microbial community composition, and soil properties

Microbial community composition explained more of the variance in GHG concentrations than did soil properties. The DBPLSR analysis revealed that microbial community composition explained 51.2%, 34.6%, and 38.0% (components 1 and 2), of variance in concentrations of CH_4, CO_2, and N_2O, respectively (Table S10). Patterns in soil properties, on the other hand, only

explained 30.0%, 31.6%, and 17.9%, of variance in concentrations of CH_4, CO_2, and N_2O, respectively, based on components 1 and 2 (Table S10).

We evaluated relationships among the variance in GHG concentrations and functional gene composition at the beginning ('start') and end of the experiment ('final') using DBPLSR. Denitrification gene composition explained 62.0% of variance in N_2O production at the start of the experiment, and 75.9% of variance in N_2O production at the end of the experiment (Table S10, components 1 and 2). Methanogenesis functional gene composition explained a higher proportion of variance in CH_4 production in 'start' samples (67.6%) than did 'final' samples (28.3%) (Table S10, components 1 and 2). 'Start' compositions of CcO and carbohydrate metabolism, explained 92.8% and 98.9% of variance in CO_2, respectively (Table S10, components 1 and 2). At the end of the experiment, CcO composition only accounted for 4.39% of variance in CO_2 production, while carbohydrate metabolism explained 77.0% of the variance in CO_2 production (Table S10, components 1 and 2).

Discussion

The presence of plants and dynamic hydrology interact to affect microbial community structure and function. This study revealed that initial hydrologic conditions (compared to manipulated hydrology) strongly influenced microbial community composition more than function. Specifically, results showed that hydrology is a strong environmental filter that determines microbial taxonomic and functional community patterns, short-term redox changes that are most distinct from historic redox conditions shift microbial communities, and plant presence can mitigate flood-induced reducing conditions and mediate greenhouse gas production.

Plant presence and dynamic hydrology influence greenhouse gas production to different degrees

Plant and hydrologic treatment strongly affected microbial function, despite hydrologic history acting as a robust environmental filter on microbial community composition. Plants can

influence GHG rates by consuming CO_2 during photosynthesis, releasing CO_2 during respiration, aerating soils in contact with roots, and releasing labile C from roots which can stimulate microbial activity (18, 20, 63). In the current study, soil redox status as visualized with IRIS tubes indicated that oxidizing conditions existed near plant roots (Fig. S1.D). This result suggested that plants can transport oxygen belowground into soils. Regardless of hydrologic history, CH_4 concentrations were highest and CO_2 concentrations were lowest in soils experiencing the wet hydrologic treatment (Fig. 4). Differences between interim and wet GHG concentrations (CH_4 and CO_2) were observed during the fifth week (July 11th, CH_4 only) and the eighth week (August 11th) of the experiment (Fig. 4, Table S3). Plant presence or absence also impacted GHG concentrations, which were generally lower across hydrologic treatments with plants. O_2 radiation from plant roots could decrease soil CH_4 flux by providing methanotrophs with needed O_2 for CH_4 consumption, thereby decreasing CH_4 emissions in the presence of plants (4, 18). However, counts of methanotrophic functional genes were low across samples. Alternatively, methanogens may be inhibited or outcompeted in the presence of O_2 (64, 65), like the conditions found near plant roots. The decline in CO_2 emissions in the presence of plants could be due to plant photosynthesis and plant uptake of atmospheric CO_2 from within the collection chamber (63). This study provides evidence that plants are important mediators of GHG production in wetland soils. Specifically, fluctuating soil moisture levels can decrease CH_4 emissions even when past environmental conditions reflect wet hydrologic histories. Therefore, both hydrology of soils and plant presence are important considerations when planning wetland restoration with the goal of enhancing soil carbon storage.

Past hydrology predicts bacterial community composition of key functional taxa

For this study, we collected wetland mesocosm soils from wet, dry, and interim hydrologic histories from a restored wetland. This change in hydrologic history resulted in different microbial community patterns with wet hydrology being the most distinct compared to microbial

communities from the dry and interim hydrology. Specifically, dry hydrologic histories were represented by taxa in the genera *Gaiella*, which are classified as strict aerobes (66). Wet hydrologic histories were uniquely identified by bacterial and archaeal taxa putatively associated with methanogenesis, methanotrophy, and iron reduction. These microbial processes occur in low redox/low oxygen systems (6). Microbes that are facultative anaerobes can shift between aerobic and anaerobic respiration based on soil redox conditions, therefore they can metabolically shift during dynamic soil hydrologic conditions. However, obligate anaerobes such as methanogens are sensitive to soil oxygen concentrations and desiccation (67). For example, in a study of peat bog layers, oxic subsurface layers contained more methanotrophs than methanogens which were found only in anoxic layers near the bottom of the bog (68). This suggests that hydrology is a strong determinant of oxygen availability in soils and that wet hydrologic histories best support microbial communities involved in anaerobic processes.

Mismatch between bacterial community composition and GHG function

The DNA-based functional gene composition explained variation in GHG concentrations measured at the beginning of the experiment more than at the end of the experiment. Hydrologic history influenced wetland soil microbial community composition more than contemporary treatments, which was emphasized in these results. The decrease in the strength of structure-function associations from the beginning of the experiment compared to the end could be due to the DNA-based molecular measurement giving insight to historical and integrated environmental conditions and not contemporary changes to redox conditions. For example, DNA from dormant and dead cells contribute to DNA-based community composition, and these relic signatures are more indicative of past than present conditions (69). Changes to functional gene composition over the eight-week experiment may have been obscured by the stable pool of dormant and relic DNA, thereby weakening structure-function relationships, as observed here for CH_4 ~ methanogenesis, CO_2 ~ central carbohydrate metabolism, and CO2 ~ cytochrome C oxidase (Table S10).

Another explanation for decreased structure-function associations could the differences in temporal resolution of DNA-based molecular methods compared to the *in situ* greenhouse gas measurements. Differential gene expression can substantially alter methane yields (70), and protein expression and activity in a variety of pathways may be altered in response to O_2 concentrations (e.g., (71), reviewed in (72)). These changes to gene expression and protein activity could alter GHG production rapidly, while changes to DNA abundance could alter GHG production over multiple microbial generations. Mesocosm microbial communities in the present study likely responded to experimental treatments (hydrology and plant presence absence) by altering gene expression and protein activity and shifting the abundance of functional genes over generations. Those slower changes to functional gene abundance were likely difficult to detect after eight weeks using DNA based methods, hence the weakening of structure-function relationships in CH_4 and CO_2 production at the end of the experiment.

Functional gene composition predicts GHG concentrations to varying degrees

Cytochrome C Oxidase

To further examine microbial functional composition and measured GHGs, we subset the metagenomic data to focus on the composition of prokaryotic cytochrome C oxidase (CcO) genes as an indicator of aerobic respiration in more oxidizing conditions. While hydrologic history significantly influenced CcO composition (PERMANOVA, R^2=0.227, P=0.001, Table S6), CcO composition was unable to explain significant variations in GHG concentrations during the eight-week incubation (Table S10, Fig. 6). This lack of explanatory power is unsurprising, given the diversity of O_2-reducing terminal oxidases, and the known presence of CcO genes in strict anaerobes (73, 74). There is no single enzyme that can be used to distinguish between aerobic and anaerobic phenotypes because aerobic and anaerobic organisms do not exist as binary groups (74). Instead, a spectrum of oxygen usage phenotypes exists (74). Evaluating the presence and number of a full suite of oxygen-utilizing enzymes may be a useful indicator of

aerobic vs. anaerobic status (74), Therefore, bioinformatic methods to facilitate this method ought to be further developed.

Central Carbohydrate Metabolism

While CcO composition was unable to explain differences in CO_2 production across treatments, the composition of central carbohydrate metabolism genes was strongly related to differences in hydrologic history, hydrologic treatment, and the production of CO_2 (Table S10, Fig. 6, Table S6). In a past study, results revealed a significant positive correlation between carbohydrate-active enzyme abundance and cumulative respiration in a tundra soil warming experiment (75). Similarly, carbohydrate metabolism genes predicted differences in soil respiration between paddy and upland soils (76). While Johnston et al. also found a relationship between CcO relative abundance and reducing conditions, this was the only study we could find that successfully used CcO genes as an indicator of redox conditions. Johnston et al. also found the total relative abundance of carbohydrate active enzyme genes to be significantly positively related to cumulative ecosystem respiration (75). The Liu et al. study identified several carbohydrate metabolism genes as significant predictors of respiration rates in upland versus paddy soils (76). While there is no single gene or defined collection of genes that have been consistently used to explain microbial community respiration responses to redox changes, various collections of carbohydrate metabolism genes may reflect differences in soil redox status and respiration (75, 76).

Denitrification

When examining denitrifier community composition and GHG production, results showed that the composition of denitrification functional genes correlated to CO_2 concentrations but not N_2O concentrations (Fig. 6). The lack of association with N_2O is unsurprising since denitrifier community composition included the suite of genes involved in the reduction of NO_3^- to N_2, with N_2O as an intermediate product that could be consumed before detection via gas chromatography. The association between denitrification and CO_2 production is likely the result

of organic denitrification, where organic matter is oxidized to CO_2 with NO_3^- as an electron acceptor (77). Organic denitrification, a form of respiratory denitrification, is typically a facultative process, found in organisms with the ability to respire aerobically when O_2 is available, and also use NO_3^- to respire anaerobically when O_2 availability decreases (78). A denitrification community-level response to soil hydrologic history and experimental drying/wetting has also been observed in a previous incubation experiment (79).

Methanogenesis

In the present study, we observed that hydrologic history (more than contemporary hydrologic treatment) influenced methanogenesis functional gene composition (Fig. 6.B, Table S6). Methanogenesis has historically been described as a specialized metabolism, in which methanogens are obligate anaerobes and obligate methanogens (meaning they do not use alternative electron acceptors to grow) (80). While atypical methanogenic pathways have recently been discovered (e.g., aerobic bacterial methane synthesis) (81), classical anaerobic methanogenesis is still recognized as the primary source of biogenic methane production (80). In the present study, our results showed a strong influence of hydrologic history on methanogen functional gene composition, which supports the classical view of methanogenesis: a specialized and strictly anaerobic metabolism was maintained in the historically wet (i.e., low O_2) field conditions, and this history dictated mesocosms' methane production capacity. The structure-function analysis (based on DBPLSR) provides another line of evidence that hydrologic history influenced methane production, where methanogen functional gene composition explained a greater proportion of variance in CH_4 production at the start of the experiment, than at the end of the experiment (Table S10).

Considering plant-microbe relationships is critical to estimating wetland carbon storage potential

Our work highlights the importance of considering plant contributions to GHG emissions. Many studies investigating GHG emissions use opaque chambers to decrease heating of the

headspace; however, these chambers can bias measurements of CH_4 emissions (63, 82). According to our study and others (63, 82), plant inclusion and plant species considerations in most cases would decrease the total estimation of CH_4 emissions from wetlands. These findings suggest that to improve estimations of C storage in wetlands, plant presence and hydrologic status should be considered to understand wetlands' potential to be a C sink.

Further, increasing extreme weather events cause changes in duration of drought or excessive rainfall, which will alter microbial ecosystem functions (83). Changes in precipitation regimes could directly alter soil hydrology or plant community composition (83). Results from this study revealed that the longer the duration of hydrologic change, the more dramatic the change in ecosystem functions. These results can be used to infer what might happen during an extreme drought event. One potential scenario is that during early summer a saturated non-tidal coastal plain wetland experiences decreased rainfall to the degree that the first meter of soil completely dries out and kills all vegetation. This may temporarily decrease CH_4 emissions, but if in the following month the same area then becomes saturated again, CH_4 emissions could increase due to the lack of vegetation. However, if the duration of drying alters the microbial community structure, then CH_4 production may be decreased upon re-flooding since obligate anaerobes will be less persistent under drier, more aerated conditions (84). This warrants future studies to more closely examine the temporal component of hydrologic changes that permanently alter microbial community structure and lead to unexpected changes to ecosystem functions.

Acknowledgments

We thank J. LeCrone, L. Armstrong, M. Stillwagon, G. Gunderson, C. Eakins, J. Basco, and C. Bledsoe for field and laboratory assistance. We thank J. Gill and the East Carolina University grounds crew for their efforts in maintaining the grounds surrounding the shade house. We also thank M. Muscarella for microbiome analyses contributions. This work was supported by the National Science Foundation (Graduate Research Fellowship Program [GRFP] grant to R.B.B.

and grant DEB #1845845 and CNH2 #2009185 to A.L.P.). The metagenomes were produced by the DOE JGI under the Community Science Program (CSP) (JGI CSP grant 503952). The work conducted by the DOE JGI, a DOE Office of Science User Facility, is supported under contract DE-AC02-05CH11231.

References

1. Kingsford RT, Basset A, Jackson L. 2016. Wetlands: conservation's poor cousins. Aquatic Conservation: Marine and Freshwater Ecosystems 26:892–916.

2. Fluet-Chouinard E, Stocker BD, Zhang Z, Malhotra A, Melton JR, Poulter B, Kaplan JO, Goldewijk KK, Siebert S, Minayeva T, Hugelius G, Joosten H, Barthelmes A, Prigent C, Aires F, Hoyt AM, Davidson N, Finlayson CM, Lehner B, Jackson RB, McIntyre PB. 2023. Extensive global wetland loss over the past three centuries. 7947. Nature 614:281–286.

3. Peralta AL, Stuart D, Kent AD, Lennon JT. 2014. A social-ecological framework for "micromanaging" microbial services. Frontiers in Ecology and the Environment 12:524–531.

4. Truu M, Juhanson J, Truu J. 2009. Microbial biomass, activity and community composition in constructed wetlands. Science of The Total Environment 407:3958–3971.

5. Mitsch WJ, Bernal B, Nahlik AM, Mander Ü, Zhang L, Anderson CJ, Jørgensen SE, Brix H. 2013. Wetlands, carbon, and climate change. Landscape Ecology 28:583–597.

6. Burgin AJ, Yang WH, Hamilton SK, Silver WL. 2011. Beyond carbon and nitrogen: how the microbial energy economy couples elemental cycles in diverse ecosystems. Frontiers in Ecology and the Environment 9:44–52.

7. Mentzer JL, Goodman RM, Balser TC. 2006. Microbial response over time to hydrologic and fertilization treatments in a simulated wet prairie. Plant and Soil 284:85–100.

8. Nygaard B, Ejrnæs R. 2009. The impact of hydrology and nutrients on species composition and richness: Evidence from a microcosm experiment. Wetlands 29:187–195.

9. Peralta AL, Ludmer S, Matthews JW, Kent AD. 2014. Bacterial community response to changes in soil redox potential along a moisture gradient in restored wetlands. Ecological Engineering 73:246–253.

10. Lennon JT, Jones SE. 2011. Microbial seed banks: The ecological and evolutionary implications of dormancy. Nature Reviews Microbiology 9:119–130.

11. Rocca JD, Hall EK, Lennon JT, Evans SE, Waldrop MP, Cotner JB, Nemergut DR, Graham EB, Wallenstein MD. 2015. Relationships between protein-encoding gene abundance and corresponding process are commonly assumed yet rarely observed. The ISME journal 9:1693–9.

12. Kim SY, Lee SH, Freeman C, Fenner N, Kang H. 2008. Comparative analysis of soil microbial communities and their responses to the short-term drought in bog, fen, and riparian wetlands. Soil Biology and Biochemistry 40:2874–2880.

13. Mitsch WJ, Gosslink JG. 2007. Wetlands, 4th ed. John Wiley & Sons, Hoboken.

14. McDonald IR, Murrell JC. 1997. The Methanol Dehydrogenase Structural Gene mxaF and Its Use as a Functional Gene Probe for Methanotrophs and Methylotrophs. FEMS Microbiology Letters 156:205–210.

15. Conrad R. 2009. The global methane cycle: recent advances in understanding the microbial processes involved. Environmental Microbiology Reports 1:285–292.

16. Kuzyakov Y. 2010. Soil Biology & Biochemistry Priming effects : Interactions between living and dead organic matter. Soil Biology and Biochemistry 42:1363–1371.

17. Philippot L, Raaijmakers JM, Lemanceau P, Van Der Putten WH. 2013. Going back to the roots: The microbial ecology of the rhizosphere. Nature Reviews Microbiology 11:789–799.

18. Chanton JP. 2005. The effect of gas transport on the isotope signature of methane in wetlands. Organic Geochemistry 36:753–768.

19. Sundberg C, Jenny JS, Tonderski K, Lindgren PE. 2007. Overland flow systems for treatment of landfill leachates-Potential nitrification and structure of the ammonia-oxidising bacterial community during a growing season. Soil Biology and Biochemistry 39:127–138.

20. Carmichael MJ, Bernhardt ES, Bräuer SL, Smith WK. 2014. The role of vegetation in methane flux to the atmosphere: should vegetation be included as a distinct category in the global methane budget? Biogeochemistry 119:1–24.

21. Hu Q, Cai J, Yao B, Wu Q, Wang Y, Xu X. 2015. Plant-mediated methane and nitrous oxide fluxes from a carex meadow in Poyang Lake during drawdown periods. Plant and Soil https://doi.org/10.1007/s11104-015-2733-9.

22. Alldred M, Baines SB. 2016. Effects of wetland plants on denitrification rates: a meta-analysis. Ecological Applications 26:676–685.

23. Ardón M, Morse JL, Doyle MW, Bernhardt ES. 2010. The Water Quality Consequences of Restoring Wetland Hydrology to a Large Agricultural Watershed in the Southeastern Coastal Plain. Ecosystems 13:1060–1078.

24. Morse JL, Ardón M, Bernhardt ES. 2012. Greenhouse gas fluxes in southeastern U.S. coastal plain wetlands under contrasting land uses. Ecological Applications 22:264–280.

25. Ardón M, Morse JL, Colman BP, Bernhardt ES. 2013. Drought-induced saltwater incursion leads to increased wetland nitrogen export. Global Change Biology 19:2976–2985.

26. Hopfensperger KN, Burgin AJ, Schoepfer VA, Helton AM. 2014. Impacts of Saltwater Incursion on Plant Communities, Anaerobic Microbial Metabolism, and Resulting Relationships in a Restored Freshwater Wetland. Ecosystems 17:792–807.

27. Jenkinson BJ, Franzmeier DP. 2006. Development and Evaluation of Iron-Coated Tubes that Indicate Reduction in Soils. Soil Science Society of America Journal 70:183–191.

28. Rabenhorst MC. 2008. Protocol for Using and Interpreting IRIS Tubes. Soil Survey Horizons 49:74–77.

29. Schneider CA, Rasband WS, Eliceiri KW. 2012. NIH Image to ImageJ: 25 years of image analysis. Nature Methods 9:671–675.

30. Mehlich A. 1984. Mehlich 3 Soil Test Extractant: A Modification of Mehlich 2 Extractant. Communications in Soil Science and Plant Analysis 15:1409–1416.

31. Mylavarapu R, Obreza T, Morgan K, Hochmuth G, Nair V, Wright A. 2014. Extraction of Soil Nutrients Using Mehlich-3 Reagent for Acid-Mineral Soils of Florida. University of Florida Institute of Food and Agricultural Science 1–7.

32. Hoffmann M, Pehle N, Huth V, Jurisch N, Sommer M, Augustin J. 2018. A simple method to assess the impact of sealing, headspace mixing and pressure vent on airtightness of manually closed chambers. Journal of Plant Nutrition and Soil Science 181:36–40.

33. Millar N, Urrea A, Kahmark K, Shcherbak I, Robertson GP, Ortiz-Monasterio I. 2018. Nitrous oxide (N2O) flux responds exponentially to nitrogen fertilizer in irrigated wheat in the Yaqui Valley, Mexico. Agriculture, Ecosystems and Environment 261:125–132.

34. Fuss R, Hueppi R. 2024. gasfluxes: Greenhouse Gas Flux Calculation from Chamber Measurements (0.6-2).

35. Hüppi R, Felber R, Krauss M, Six J, Leifeld J, Fuß R. 2018. Restricting the nonlinearity parameter in soil greenhouse gas flux calculation for more reliable flux estimates. PLOS ONE 13:e0200876.

36. Bledsoe R, Goodwillie C, Peralta A. 2020. Long-Term Nutrient Enrichment of an Oligotroph-Dominated Wetland Increases Bacterial Diversity in Bulk Soils and Plant Rhizospheres. mSphere 5.

37. Goodwillie C, McCoy MW, Peralta AL. 2020. Long-term nutrient enrichment, mowing, and ditch drainage interact in the dynamics of a wetland plant community. Ecosphere 11:e03252.

38. Caporaso JG, Lauber CL, Walters W a, Berg-Lyons D, Huntley J, Fierer N, Owens SM, Betley J, Fraser L, Bauer M, Gormley N, Gilbert J a, Smith G, Knight R. 2012. Ultra-high-throughput microbial community analysis on the Illumina HiSeq and MiSeq platforms. The ISME Journal 6:1621–1624.

39. Apprill A, Mcnally S, Parsons R, Weber L. 2015. Minor revision to V4 region SSU rRNA 806R gene primer greatly increases detection of SAR11 bacterioplankton. Aquatic Microbial Ecology 75:129–137.

40. Parada AE, Needham DM, Fuhrman JA. 2016. Every base matters: Assessing small subunit rRNA primers for marine microbiomes with mock communities, time series and global field samples. Environmental Microbiology 18:1403–1414.

41. Schloss PD, Westcott SL, Ryabin T, Hall JR, Hartmann M, Hollister EB, Lesniewski R a., Oakley BB, Parks DH, Robinson CJ, Sahl JW, Stres B, Thallinger GG, Van

Horn DJ, Weber CF. 2009. Introducing mothur: Open-source, platform-independent, community-supported software for describing and comparing microbial communities. Applied and Environmental Microbiology 75:7537–7541.

42. Kozich JJ, Westcott SL, Baxter NT, Highlander SK, Schloss PD. 2013. Development of a dual-index sequencing strategy and curation pipeline for analyzing amplicon sequence data on the miseq illumina sequencing platform. Applied and Environmental Microbiology 79:5112–5120.

43. Quast C, Pruesse E, Yilmaz P, Gerken J, Schweer T, Yarza P, Peplies J, Glöckner FO. 2013. The SILVA ribosomal RNA gene database project: Improved data processing and web-based tools. Nucleic Acids Research 41:590–596.

44. Rognes T, Flouri T, Nichols B, Quince C, Mahé F. 2016. VSEARCH: a versatile open source tool for metagenomics. PeerJ 4:e2584.

45. Schloss PD. 2021. Amplicon Sequence Variants Artificially Split Bacterial Genomes into Separate Clusters. mSphere 6:e00191-21.

46. Glassman SI, Martiny JBH. 2018. Broadscale Ecological Patterns Are Robust to Use of Exact Sequence Variants versus Operational Taxonomic Units. mSphere 3:e00148-18.

47. Peralta AL, Bledsoe RB, Muscarella ME, Huntemann M, Clum A, Foster B, Foster B, Roux S, Palaniappan K, Varghese N, Mukherjee S, Reddy TBK, Daum C, Copeland A, Chen I-MA, Ivanova NN, Kyrpides NC, Glavina del Rio T, Eloe-Fadrosh EA. 2020. Metagenomes from Experimental Hydrologic Manipulation of

Restored Coastal Plain Wetland Soils (Tyrell County, North Carolina). Microbiol Resour Announc 9.

48. Chen I-MA, Markowitz VM, Chu K, Palaniappan K, Szeto E, Pillay M, Ratner A, Huang J, Andersen E, Huntemann M, Varghese N, Hadjithomas M, Tennessen K, Nielsen T, Ivanova NN, Kyrpides NC. 2017. IMG/M: integrated genome and metagenome comparative data analysis system. Nucleic Acids Research 45:D507–D516.

49. Huntemann M, Ivanova NN, Mavromatis K, Tripp HJ, Paez-Espino D, Tennessen K, Palaniappan K, Szeto E, Pillay M, Chen I-MA, Pati A, Nielsen T, Markowitz VM, Kyrpides NC. 2016. The standard operating procedure of the DOE-JGI Metagenome Annotation Pipeline (MAP v.4). Standards in Genomic Sciences 11:17.

50. Markowitz VM, Chen I-MA, Chu K, Szeto E, Palaniappan K, Pillay M, Ratner A, Huang J, Pagani I, Tringe S, Huntemann M, Billis K, Varghese N, Tennessen K, Mavromatis K, Pati A, Ivanova NN, Kyrpides NC. 2014. IMG/M 4 version of the integrated metagenome comparative analysis system. Nucleic Acids Research 42:D568–D573.

51. R Core Team. 2019. R: A language and environment for statistical computing. R Foundation for Statistical Computing, Vienna, Austria.

52. Oksanen J. 2015. Vegan : ecological diversity 1:1–12.

53. Roberts D. 2016. Package ‘ labdsv .’ 1.8–0.

54. Bates D, Machler M, Bolker B, Walker S. 2015. Fitting Linear Mixed-Effects Models Using lme4. Journal of Statistical Software 67:1–48.

55. Hurvich C, Tsai C. 1993. A CORRECTED AKAIKE INFORMATIONON CRITERION FOR VECTOR AUTOREGRESSIVE MODEL SELECTION. Journal of Time Series Analysis 14:271–279.

56. Gorsky AL, Racanelli GA, Belvin AC, Chambers RM. 2019. Greenhouse gas flux from stormwater ponds in southeastern Virginia (USA). Anthropocene 28.

57. Barton K. 2019. Package “MuMIn.” R Package Version 1.43.15.

58. Schielzeth H, Dingemanse NJ, Nakagawa S, Westneat DF, Allegue H, Teplitsky C, Réale D, Dochtermann NA, Garamszegi LZ, Araya-Ajoy YG. 2020. Robustness of linear mixed-effects models to violations of distributional assumptions. Methods in Ecology and Evolution 11:1141–1152.

59. Blanca MJ, Alarcón R, Arnau J, Bono R, Bendayan R. 2017. Non-normal data: Is ANOVA still a valid option? Psicothema 29:552–557.

60. Havlicek LL, Peterson NL. 1974. Robustness of the T Test: A Guide for Researchers on Effect of Violations of Assumptions. Psychol Rep 34:1095–1114.

61. Schneider G, Chicken E, Becvarik R. 2023. NSM3: Functions and Datasets to Accompany Hollander, Wolfe, and Chicken - Nonparametric Statistical Methods, Third Edition (1.18).

62. Boj E, Caballe A, Delicado P, Fortiana J. 2017. Package ‘ dbstats .’ R Package Version 1.0.5.

63. Luan J, Wu J. 2014. Gross photosynthesis explains the “artificial bias” of methane fluxes by static chamber (opaque versus transparent) at the hummocks in a boreal peatland. Environmental Research Letters 9.

64. Bethke CM, Sanford RA, Kirk MF, Jin Q, Flynn TM. 2011. The thermodynamic ladder in geomicrobiology. American Journal of Science 311:183–210.

65. Cedervall PE, Dey M, Pearson AR, Ragsdale SW, Wilmot CM. 2010. Structural Insight into Methyl-Coenzyme M Reductase Chemistry Using Coenzyme B Analogues,. Biochemistry 49:7683–7693.

66. Albuquerque L, França L, Rainey FA, Schumann P, Nobre MF, Da Costa MS. 2011. Gaiella occulta gen. nov., sp. nov., a novel representative of a deep branching phylogenetic lineage within the class Actinobacteria and proposal of Gaiellaceae fam. nov. and Gaiellales ord. nov. Systematic and Applied Microbiology 34:595–599.

67. Fetzer S, Bak F, Conrad R. 1993. Sensitivity of methanogenic bacteria from paddy soil to oxygen and desiccation. FEMS Microbiology Ecology 12:107–115.

68. Lew S, Glińska-Lewczuk K. 2018. Environmental controls on the abundance of methanotrophs and methanogens in peat bog lakes. Science of the Total Environment 645:1201–1211.

69. Lennon JT, Muscarella ME, Placella SA, Lehmkuhl BK. 2018. How, When, and Where Relic DNA Affects Microbial Diversity. mBio 9:10.1128/mbio.00637-18.

70. Shi W, Moon CD, Leahy SC, Kang D, Froula J, Kittelmann S, Fan C, Deutsch S, Gagic D, Seedorf H, Kelly WJ, Atua R, Sang C, Soni P, Li D, Pinares-Patiño CS, McEwan JC, Janssen PH, Chen F, Visel A, Wang Z, Attwood GT, Rubin EM. 2014. Methane yield phenotypes linked to differential gene expression in the sheep rumen microbiome. Genome Res 24:1517–1525.

71. Lynch AS, Lin EC. 1996. Transcriptional control mediated by the ArcA two-component response regulator protein of Escherichia coli: characterization of DNA binding at target promoters. Journal of Bacteriology 178:6238–6249.

72. Saleh-Lakha S, Miller M, Campbell RG, Schneider K, Elahimanesh P, Hart MM, Trevors JT. 2005. Microbial gene expression in soil: methods, applications and challenges. Journal of Microbiological Methods 63:1–19.

73. Esposti MD. 2020. On the evolution of cytochrome oxidases consuming oxygen. Biochimica et Biophysica Acta (BBA) - Bioenergetics 1861:148304.

74. Jabłońska J, Tawfik DS. 2019. The number and type of oxygen-utilizing enzymes indicates aerobic vs. anaerobic phenotype. Free Radical Biology and Medicine 140:84–92.

75. Johnston ER, Hatt JK, He Z, Wu L, Guo X, Luo Y, Schuur EAG, Tiedje JM, Zhou J, Konstantinidis KT. 2019. Responses of tundra soil microbial communities to half a

decade of experimental warming at two critical depths. Proceedings of the National Academy of Sciences 116:15096–15105.

76. Liu Y-R, Delgado-Baquerizo M, Yang Z, Feng J, Zhu J, Huang Q. 2020. Microbial taxonomic and functional attributes consistently predict soil CO2 emissions across contrasting croplands. Science of The Total Environment 702:134885.

77. Dlamini JC, Chadwick D, Hawkins JMB, Martinez J, Scholefield D, Ma Y, Cárdenas LM. 2020. Evaluating the potential of different carbon sources to promote denitrification. The Journal of Agricultural Science 158:194–205.

78. Tiedje JM, Simkins S, Groffman PM. 1989. Perspectives on measurement of denitrification in the field including recommended protocols for acetylene-based methods. Plant Soil 115:261–284.

79. Peralta AL, Ludmer S, Kent AD. 2013. Hydrologic history influences microbial community composition and nitrogen cycling under experimental drying/wetting treatments. Soil Biology and Biochemistry 66:29–37.

80. Lyu Z, Shao N, Akinyemi T, Whitman WB. 2018. Methanogenesis. Current Biology 28:R727–R732.

81. Wang Q, Alowaifeer A, Kerner P, Balasubramanian N, Patterson A, Christian W, Tarver A, Dore JE, Hatzenpichler R, Bothner B, McDermott TR. 2021. Aerobic bacterial methane synthesis. PNAS 118.

82. Günther A, Jurasinski G, Huth V, Glatzel S. 2014. Opaque closed chambers underestimate methane fluxes of Phragmites australis (Cav.) Trin. ex Steud. Environmental Monitoring and Assessment 186:2151–2158.

83. Jansson JK, Hofmockel KS. 2020. Soil microbiomes and climate change. Nat Rev Microbiol 18:35–46.

84. Angel R, Claus P, Conrad R. 2012. Methanogenic archaea are globally ubiquitous in aerated soils and become active under wet anoxic conditions. ISME J 6:847–862.

Figures and Tables

Figure 1

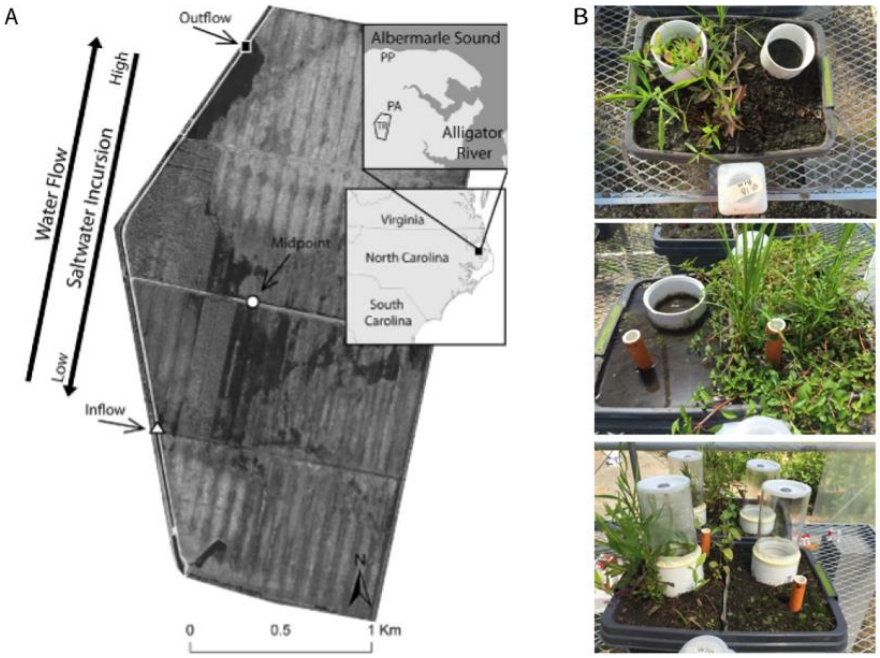

Figure 1. Field site and mesocosm set-up. Wetland mesocosms sourced from the Timberlake Observatory for Wetland Restoration (image modified from Ardón et al., 2013) (A). Aerial view of wetland mesocosm setup, where the left side of box represents plant treatment, and right side represents no plant treatment separated by a stainless mesh divider (B, top). PVC collars installed for measuring greenhouse gas concentrations. Also shown is a 1-liter bottle attached to each side of the mesocosm used to maintain water levels. Example of a wet treatment mesocosm with IRIS tubes installed (B, middle). Example of mesocosm with prepared for GHG sampling (B, bottom).

Figure 2

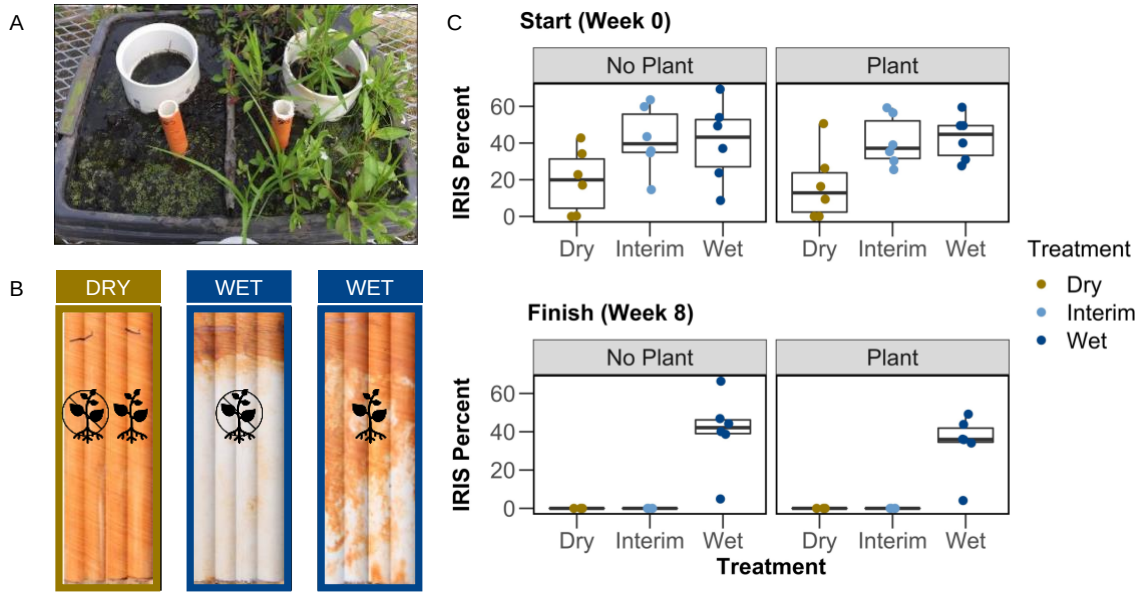

Figure 2. Indicator of reduction in soils (IRIS) tubes mesocosm image (A), IRIS tube example image (B), and boxplots summarizing redox status at the beginning and end of experiment (C). Percent paint removed from IRIS tubes at start of experiment (week 0) and the end of experiment (week 8). Example IRIS tubes used for ImageJ analysis post-incubation (B) with plant icons crossed out represent IRIS tubes from mesocosms with plants removed and plant icons represent IRIS tubes from mesocosm with plants present. Box plots summarize percent paint removed from IRIS tubes at start (week 0) and finish (week 8) of experimental incubation. Color represents hydrologic treatment: brown = dry, light blue = interim, dark blue = wet. Individual samples are plotted as points and colored by hydrologic treatment. Boxplots summarize median, first and third quartiles, and two whiskers extending |≤| 1.5 * interquartile range.

Table 1. Soil chemical and physical properties measured after eight weeks of hydrologic manipulation. Average (mean ± standard deviation) by hydrologic treatment and plant status reported. Abbreviations: MDL = Below detection limit.

History	Dry		Interim		Wet	
Plant	No Plant	Plant	No Plant	Plant	No Plant	Plant
Moisture (%)	39 ± 0.31	14 ± 0.03	19 ± 0.16	13 ± 0.02	29 ± 0.23	62 ± 0.07
pH	5.31 ± 0.11	5.31 ± 0.09	5.4 ± 0.16	5.35 ± 0.1	5.55 ± 0.15	5.41 ± 0.17
NH_4^+ mg L^{-1}	0.39 ± 0.07	0.27 ± 0.04	0.26 ± 0.1	0.19 ± 0.02	0.77 ± 0.76	0.39 ± 0.42
NO_3^- mg L^{-1}	0.08 ± 0.07	MDL	0.25 ± 0.38	MDL	0.01 ± 0.0005	MDL
Total C (%)	4.63 ± 0.78	4.63 ± 0.81	4.48 ± 0.32	4.37 ± 0.52	4.91 ± 0.92	4.68 ± 0.74
Total N (%)	0.22 ± 0.03	0.22 ± 0.03	0.22 ± 0.01	0.21 ± 0.03	0.24 ± 0.04	0.23 ± 0.03
P ppm	21.00 ± 4.14	20.41 ± 4.4	23.58 ± 8.87	22.83 ± 8.37	23.16 ± 5.98	23 ± 5.79
K ppm	33.66 ± 5.97	30.25 ± 10.31	39.5 ± 11.44	26.75 ± 3.04	46.16 ± 16.02	34.25 ± 10.78
Mg ppm	77.58 ± 6.46	74.66 ± 11.43	86 ± 22.33	78.66 ± 16.47	89.25 ± 16.85	79.41 ± 18.8
S ppm	15.75 ± 1.94	15.33 ± 2.29	13.25 ± 1.25	12.16 ± 0.40	11.33 ± 1.21	11.5 ± 1.00
Fe ppm	252.66 ± 14.45	243.66 ± 17.06	275.33 ± 27.07	251.16 ± 37.6	306.83 ± 22.52	280.66 ± 40.71
Mn ppm	3.91 ± 1.15	3.41 ± 0.97	4.33 ± 1.16	4.58 ± 1.31	5.83 ± 1.32	5.58 ± 2.05
Humic matter (%)	2.35 ± 0.19	2.17 ± 0.14	2.04 ± 0.29	2.28 ± 0.22	1.98 ± 0.422	1.96 ± 0.43

Figure 3

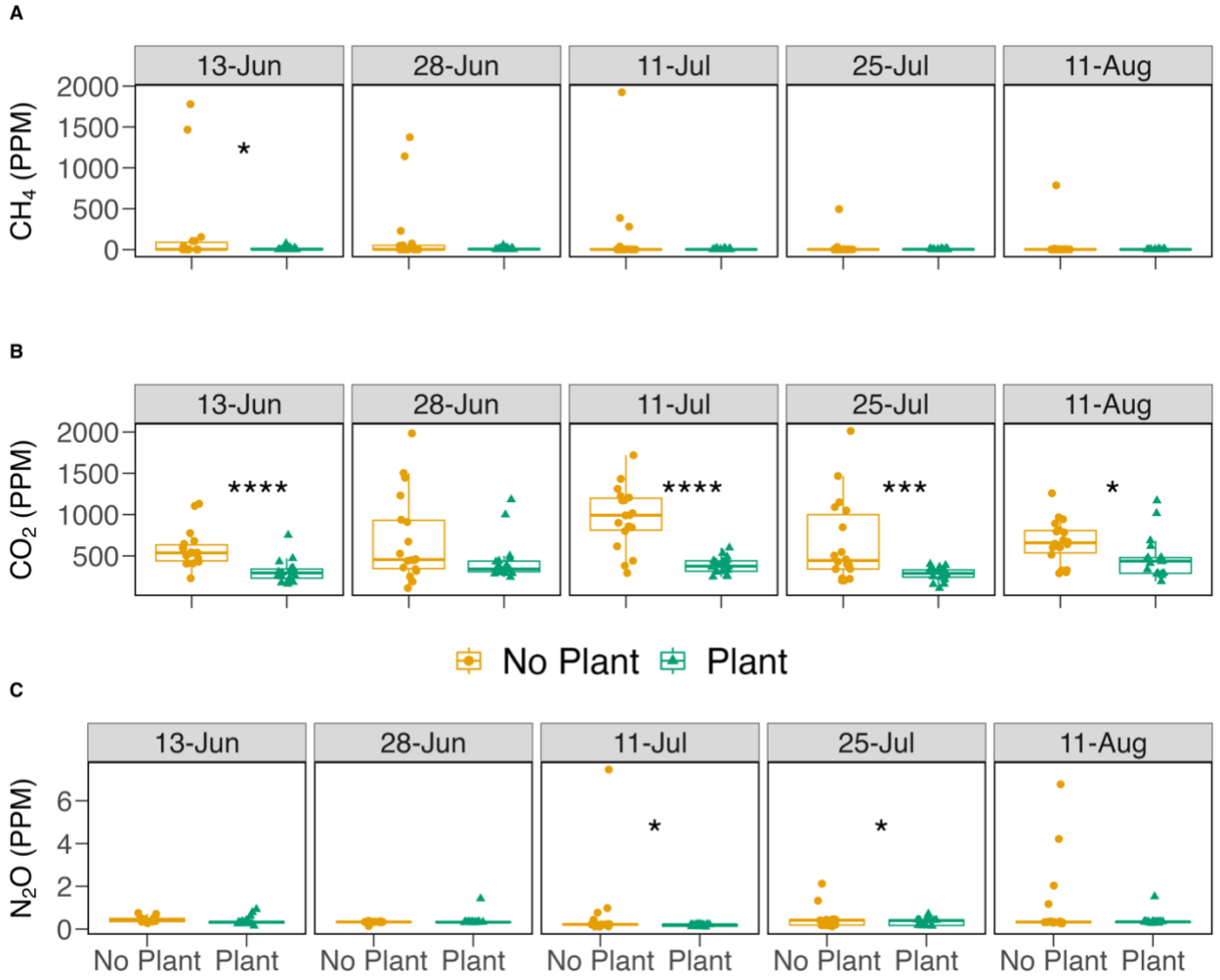

Figure 3. Greenhouse gas concentrations comparing no plant vs. plant treatments. Concentrations are in parts per million (PPM) of CH_4 (panel A), CO_2 (panel B), and N_2O (panel C) are compared for plant presence/absence treatments during five timepoints. Color represents plant presence/absence: orange = no plant, green = plant. Individual samples are plotted as points and colored by hydrologic treatment. Boxplots summarize median, first and third quartiles, and two whiskers extending |≤| 1.5 * interquartile range. Asterisks represent significance levels of Wilcoxon Rank-Sum tests (****: $p \leq 0.0001$, ***: $p \leq 0.001$, **: $p \leq 0.01$, *: $p \leq 0.05$, no symbol: $p > 0.05$).

Figure 4

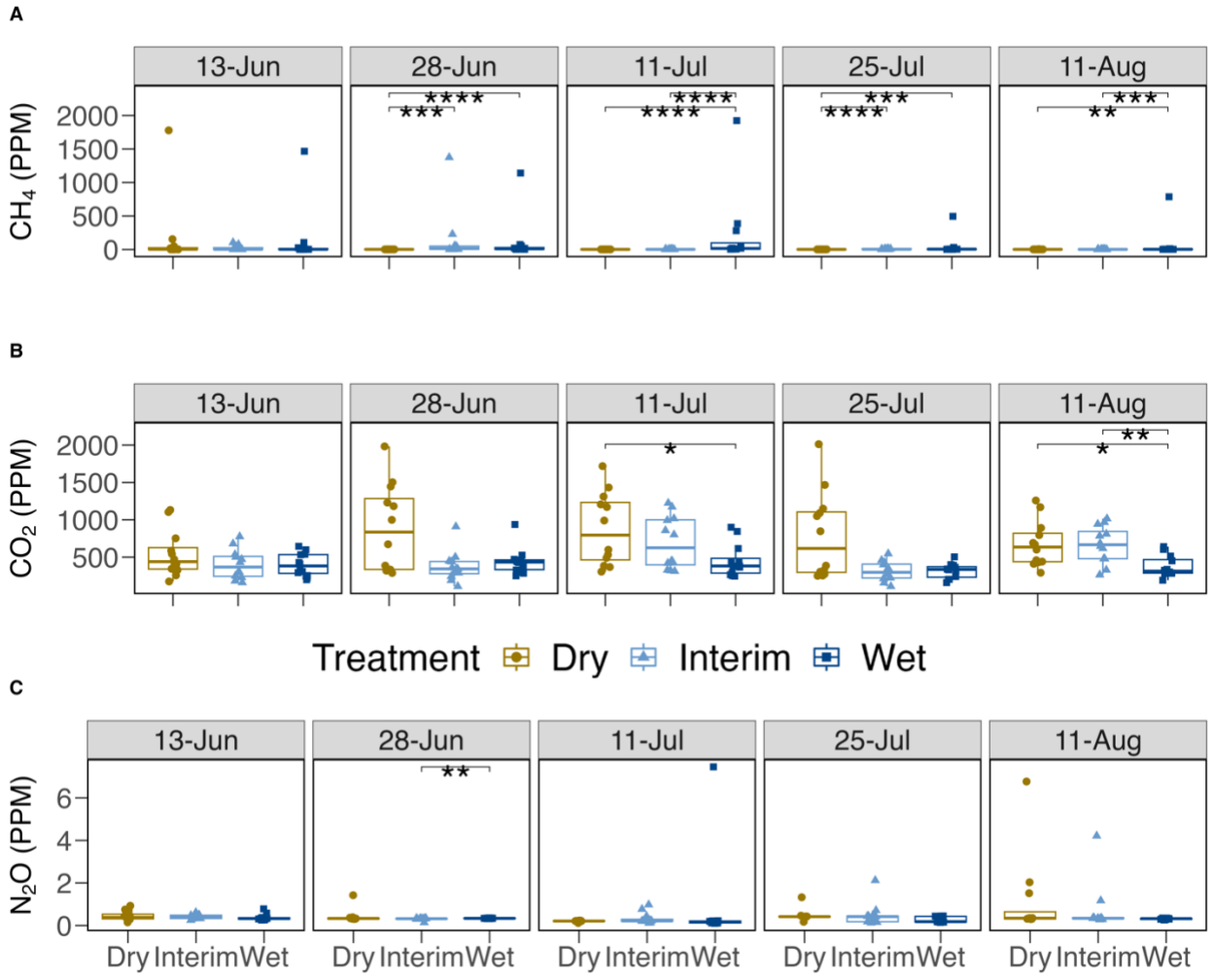

Figure 4. Greenhouse gas concentrations in dry, interim, and wet hydrologic treatments. Concentrations are in parts per million (PPM) of CH_4 (panel A), CO_2 (panel B), and N_2O (panel C) are compared for hydrologic treatments during five timepoints. Color represents hydrologic treatment: brown = dry, light blue = interim, dark blue = wet. Individual samples are plotted as points and colored by hydrologic treatment. Boxplots summarize median, first and third quartiles, and two whiskers extending |≤| 1.5 * interquartile range. Asterisks represent significance levels of Dwass, Steel, Critchlow, and Fligner (SDCFlig) tests (****: $p \leq 0.0001$, ***: $p \leq 0.001$, **: $p \leq 0.01$, *: $p \leq 0.05$, no symbol: $p > 0.05$).

Figure 5

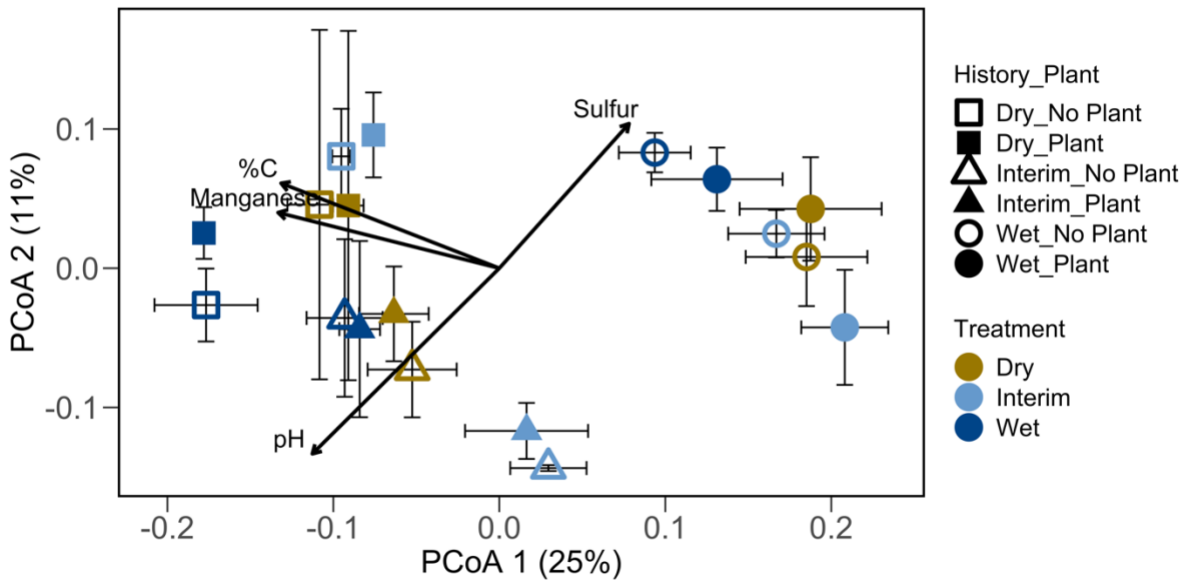

Figure 5. Ordination based on a principal coordinates analysis (PCoA) depicting community composition of the bacterial and archaeal community composition based on the 16S rRNA gene. Colors refer to hydrologic treatments: brown = dry, light blue = interim, dark blue = wet. Shapes refer to hydrologic history of the sample: square = dry, triangle = interim, circle = wet. Open shapes refer to samples from mesocosms without plants, while closed shapes refer to samples from mesocosms with plants. Labelled vectors represent relationships among soil physiochemical variables and the microbial community ordination with $P \leq 0.05$, scaled by their correlation (using the envfit function).

Figure 6

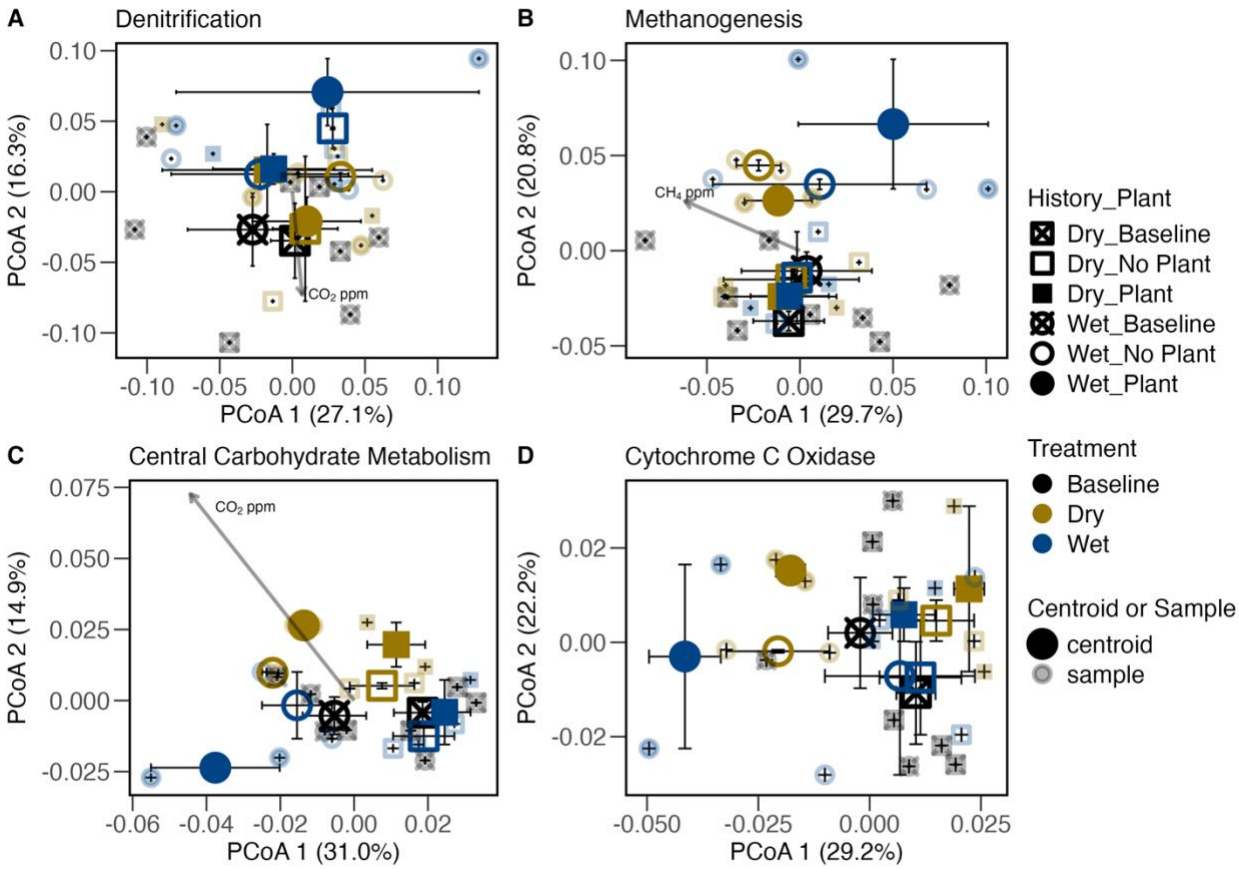

Figure 6. Ordination based on a principal coordinates analysis (PCoA) depicting community composition of the functional gene modules. The PCoA ordination is based on the Bray-Curtis distance of relative abundance of functional genes within respective KEGG modules: Panel A: Denitrification (KEGG Module M00529), B: Methanogen (M00617), C: Central Carbohydrate Metabolism (M00001-M00011, M00307-M00309, M00580, and M00633), D: Prokaryotic Cytochrome C Oxidase (M00155). Colors refer to hydrologic treatments: black = baseline, brown = dry, dark blue = wet. Shapes refer to hydrologic history of the sample: square = dry, triangle = interim, circle = wet. The shape fill represents plant treatment: cross = baseline, open = no plant, closed = plant. Baseline samples were collected before the start of hydrologic and plant treatments. Large, dark, opaque points represent centroids of samples within a group,

while individual samples are represented by smaller transparent points. Vectors represent significant ($P \leq 0.1$) relationships among greenhouse gas concentrations and functional gene composition, with the length of the vectors scaled by the strength of correlation (using the envfit function).